Int. J. Nanoelectronics and Materials **3** (2010) 87-97

Structural and optical properties of calcium-doped zinc oxide sputtered from nanopowder target materials

Z. Ben Ayadi[1,*], L. El Mir[1], J. El Ghoul[1], K. Djessas[2], S. Alaya[1]

[1]*Laboratoire de Physique des Matériaux et des Nanomatériaux appliquée àl'Environnement, Faculté des Sciences de Gabès, Cité Erriadh Manara Zrig, 6072 Gabès, Tunisie.*
[2]*Laboratoire Procédés, Matériaux et Energie Solaire (PROMES-CNRS), Université de Perpignan, Rambla de la thermodynamique, Tecnosud, 66100 Perpignan Cedex, France.*

Abstract

Calcium-doped zinc oxide (ZnO:Ca) thin films were deposited onto glass substrates by rf-magnetron sputtering at ambient temperature using nanocrystalline powder synthesized by the sol-gel method. The structural, electrical and optical properties of films as a function of Ca concentration were investigated. Ca-doped films exhibit high optical transparency in the visible and near infrared region. A minimum resistivity of 2.3×10^{-3} Ωcm, was obtained for the film doped with 3.0 at.% of calcium. Due to their good optical and electrical properties, ZnO:Ca films are promising candidates for their use as transparent electrodes in solar cells.

Keywords: Nanoparticles, Sol-gel, Magnetron sputtering, Solar cells.
PACS: 78.67.Bf, 81.20.Fw, 81.40.Rs, 88.40.H-.

[*]) For correspondence; Email: Zouhaier.BenAyadi@fsg.rnu.tn.

1. Introduction

ZnO is one of the most promising materials for its optical and electrical properties, in comparison with other transparent conducting oxides (TCOs) like indium tin oxide (ITO) and tin oxide (SnO_2) [1-3]. The other advantages of ZnO films are their low cost, non-toxicity, high band gap, ease of doping and excellent durability under hydrogen atmosphere. The electrical and optical properties depend on film composition, structure, crystallinity and dopants concentration.

ZnO thin films were prepared by different techniques of deposition: sputtering [4], laser [5], evaporation [6], spray [7], chemical vapor deposition [8] and sol-gel [9, 10]. However, among these techniques, sputtering and sol-gel processes offered much more advantages. Sputtering performs high deposition rate, good film properties and process stability. On the other hand, sol-gel technology emerged within the last two decades and quickly became one of the most important and promising new material fabrication methods. Indeed, besides the fact that it is a low cost technique, it enables researchers to easily design and fabricate a wide variety of different materials, including the possibility of doping even at high level concentrations.

Up to now, we have fabricated doped and co-doped ZnO TCOs thin films by rf-magnetron sputtering from aerogel nanoparticles as target materials [11-14]. In the present paper, we report the influence of dopant concentration (Ca) on the structural, electrical and optical properties of ZnO:Ca thin films for the first time.

2. Experimental details

ZnO:Ca aerogels nanoparticles were prepared by the sol-gel method. The synthesis procedure of ZnO:Ca is as follows: 16 g zinc acetate dehydrate [$Zn(CH_3COO)_2.2H_2O$] was dissolved in 112 ml methanol, and magnetic stirring dispersed to form a mixture. Different additions of calcium chloride-6-hydrate [$CaCl_2$, $6H_2O$] were added into the mixture according to [Ca]/[Zn] ratios of 0.01, 0.02, 0.03, 0.04. After an additional 15 min under magnetic stirring, the solution was placed in an autoclave and dried in supercritical condition of ethyl alcohol (EtOH). The ZnO:Ca thin films were

deposited onto glass substrates by rf-magnetron sputtering equipped with an r.f. generator operating at 13.56 MHz. The sputtering targets were prepared from the aerogel nanoparticles, which had not been pressed nor sintered. The target-to-substrates distance was fixed at 75 mm. Before depositing of the ZnO:Ca thin films, the substrates were ultrasonically cleaned in HCl, rinsed in deionized water, then subsequently in ethanol and rinsed again. The substrates were placed inside the chamber and then evacuated to a base pressure of 6×10^{-5} Pa. Then, a controlled flux of 6 N pure argon gas was introduced into the chamber to act as sputter gas and the sputtering power during deposition was 25 W. All the films were deposited at room temperature and the target was water-cooled. The substrate surface was monitored by thermocouple during sputter deposition. Although the substrate glasses were not intentionally heated, the surface substrate temperature reached about 50°C.

The structural properties of the aerogel powders and the thin films were determined by X-ray diffraction (XRD) using a Cu Kα radiation (1.5418 Å). The aerogel powders were, also, characterized by the transmission of electron microscopy (TEM), using the JEM-200CX microscope. The thickness of the films was measured using a Tencor profilometer. Electrical resistivity, Hall mobility and carrier concentration were measured at room temperature by Hall measurement with the Van der Pauw method. The optical transmittance of the films was determined using Shimadzu UV-3101 PC spectrophotometer in the wavelength range from 200 to 2500 nm. For transmittance measesurement, the beam was made to enter the film through the glass substrate and a blank glass slide was kept in the path of the reference beam for compensation.

3. Results and discussion

Figure 1 shows TEM photograph of the aerogel powders of ZnO:Ca as prepared by sol-gel method. The crystallites present a very similar prismatic shape with a narrow particle size distribution. The majority of ZnO particles present in this powder have a size between 20 and 30 nm.

Figure 2 shows the XRD patterns of the aerogel powders with varying calcium concentration of 1-4 at.%. Three pronounced ZnO diffraction peaks, (100), (002) and (101) appear at 2θ = 31.73°,

33.40° and 35.21° respectively, which are very close to wurtzite ZnO ones [15]. This result indicates that ZnO:Ca aerogel powder has a polycrystalline hexagonal wurtzite structure. Diffraction lines of ZnO were broad, and diffraction broadening was found to be dependent on Miller indices of the corresponding sets of crystal planes. For our samples, the (002) diffraction line was more narrower than the (101) line, which is in turn more broader than the (100) line. This indicated an asymmetry in the crystallite shape. It was supposed that crystallites were in the form of cylinder (prism), having the height (direction of the crystal *c*-axis) bigger than the basal diameter (crystal axes, *a* and *b*). The average grain size was calculated using Scherrer's formula [16]:

$$G = \frac{0{,}9\lambda}{B\cos\theta_B} \qquad (1)$$

where is θ the X-ray wavelength (1.5418 Å), θ_B is the maximum of the Bragg diffraction peak (in radians) and θ is the line width at half maximum. The average grain size of the basal diameter of the cylinder-shape crystallites varies from 20 nm to 30 nm, whereas the height of the crystallites from 30 nm to 40 nm. On the other hand, the XRD spectra indicated another phase that is $Ca(OH)_2Zn(OH)_2$ for nanopowders doped with 4.0 at.% of Ca concentration.

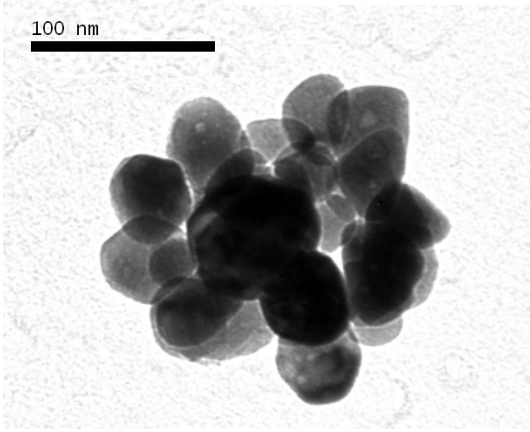

Fig. 1: Typical TEM photograph showing the general morphology of ZnO:Ca aerogel nanoparticles.

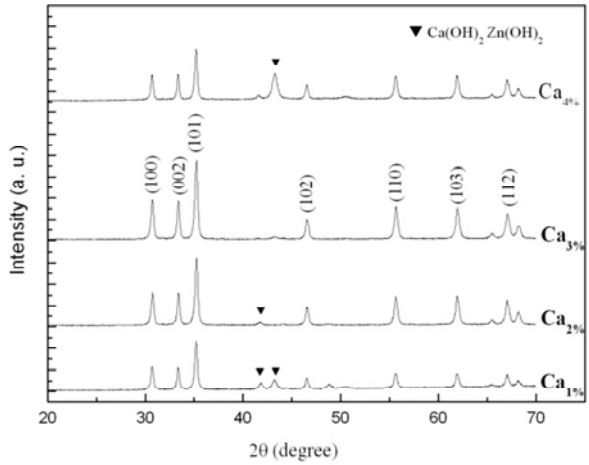

Fig. 2: X-ray diffraction patterns of Ca-doped ZnO aerogel nanoparticles.

XRD patterns of ZnO:Ca thin films deposited by rf-magnetron sputtering on glass substrates are shown in Figure 3. It shows that all films are crystalline and exhibit the hexagonal structure (JCPDS 36-1451) with the *c*-axis oriented preferentially normal to the substrate surface. From the XRD results, it is concluded that the film properties are strongly dependent on calcium concentration. The grain sizes for the films, calculated using Scherrer's formula, are comparable to those of the ZnO powder. A small deviation in (002) peak was found when the concentration was varied (see table 1), indicating that some residual stress inside the film may exist [3]. The variation of the (002) interreticular distance *d* (see table 1), shows that all the sputtered thin films *d* values are larger than that of ZnO powder which is equal to 0.2603 nm. These results from the deterioration of the film crystallinity may be due to the formation of the stresses by the difference in ion size between zinc and the dopant and the segregation of dopants in grain boundaries [17-19]. The 3.0 at.% of Ca doping is critical to have high quality ZnO thin films. The (002) peak intensity increases with the calcium concentration and reach a maximum for a concentration of 3.0 at.% of Ca. The thickness of the film was approximately 500 nm, such value is measured by Tencor profilometer measurement.

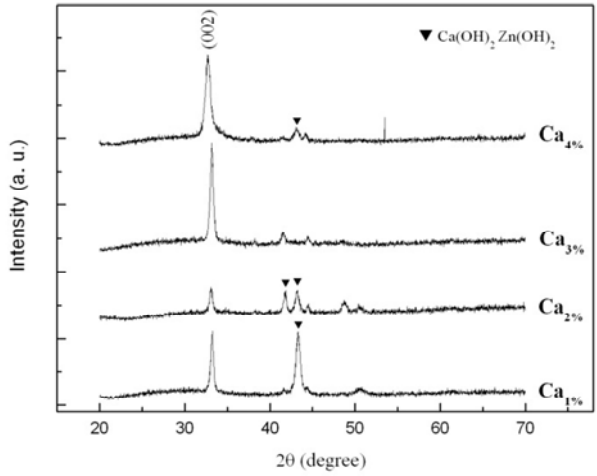

Fig. 3: X-ray diffraction patterns of ZnO:Ca thin films at different dopant concentrations.

Table 1:Variation of the (002) peak positions, FWHM, grain size and interreticular distance (*d*) of ZnO:Ca films with different Ca concentrations.

at.% Ca	(002), 2θ (deg.)	Grain size (nm)	d (nm)	E_g (eV)
1	33.21	33.21	0.270	3.31
2	33.06	33.06	0.271	3.32
3	33.16	33.16	0.269	3.33
4	32.72	32.72	0.273	3.36

The variations of the resistivity (ρ), carrier concentration (n) and Hall mobility (μ) of Ca-doped ZnO films with doping concentration are shown in Figure 4. All our results were confirmed to be n type by Hall measurements and films exhibited semiconducting behaviour. The resistivity found to decrease initially with increasing Ca content up to 3.0 at.% where the film resistivity becomes a minimum of 2.3 $\times 10^{-3}$ Ωcm. The decrease in resistivity with doping concentration is due to improvement in crystallinity. The mobility is found to increase

with doping concentration, which is also due to improvement in crystalline structure. However, the resistivity of films increases with a further increase in the Ca content up to 4.0 at.%. It is also seen in Figure 4 that Hall mobility of films decreases with increasing the Ca doping concentration (>3.0 at.%). This may be attributed to a decrease in the grain size of films with increasing Ca doping concentration because the decrease in the grain size increases the grain boundary scattering thus decreasing the hall mobility [20]. It is well known that the n-type conductivity of undoped ZnO is caused by the presence of intrinsic defects such as oxygen vacancies and interstitial zinc [21, 22]. The incorporation of Ca into ZnO improves the electrical conductivity due to the creation of one extra carrier as a result of substitutional doping of Ca^{2+} at Zn^{2+} sites. On the other hand, the increase of carrier concentration indicates that calcium doping atoms are effectively incorporated substitutionally at zinc sites in ZnO lattice.

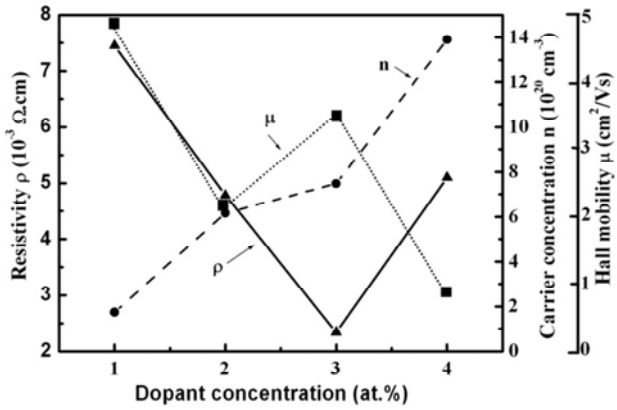

Fig. 4: Resistivities, Hall mobility and carrier concentration of ZnO:Ca thin films as a function of the dopant concentration.

Figure 5 represents the optical spectra of ZnO:Ca films, in the wavelength range of 250 nm to 2500 nm. The transmittance within the visible and the near infrared region is always higher than 90%. They exhibit sharp ultraviolet absorption edges at about $\lambda \sim 348$-354 nm are higher than the intrinsic band gap (3.2 eV) of ZnO. The

transmittance falls sharply at the band edge which is an indication of the good films crystallinity. A weak fluctuation in the spectrum is mainly caused by interference phenomenon between the top and bottom surface of the films. This indicates that the films have a smooth surface. In a direct transition semiconductor like ZnO, the absorption coefficient α is related to the optical energy band gap E_g for high photon energies as [23]:

$$\alpha(h\nu) = C\left(h\nu - E_g\right)^{\frac{1}{2}} \tag{2}$$

where C is a constant for direct transition, and $h\nu$ is the energy of the incident photon. The plot of $(\alpha h\nu)^2$ against $(h\nu)$ shows a linear dependence. This means that ZnO films are direct transition type semiconductor. The band gap E_g is determined by extrapolating the linear part of the spectrum $(\alpha h\nu)^2$ curve towards the $(h\nu)$ axis. We see that the band gap of ZnO:Ca films varies from 3.31 to 3.36 eV (see table 1). As shown in the literature, the direct optical band gap of pure polycrystalline ZnO film is 3.28-3.30 eV. We attribute the slightly higher band gap of our ZnO:Ca films to the Burstein-Moss effect caused by an increased free electron concentration due to the Ca doping [24, 25].

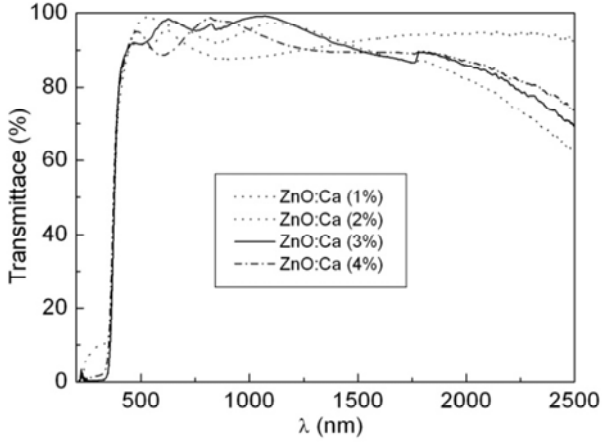

Fig. 5: The transmission in the UV-Vis-IR regions of ZnO:Ca thin films with various Ca concentrations.

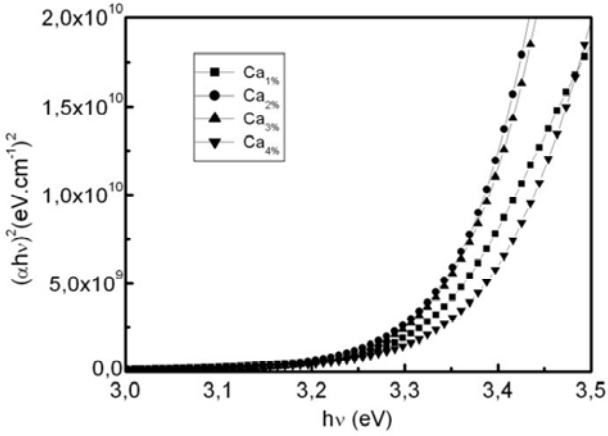

Fig. 6: Plots or $(\alpha h\nu)^2$ vs. Photon energy $h\nu$ of ZnO:Ca thin films with various Ca concentrations.

4. Conclusion

ZnO:Ca thin films were deposited onto glass substrates by rf-magnetron sputtering at ambient temperature using nanocrystalline powder synthesized by the sol-gel method. Structural, electrical and optical properties were investigated to explore a possibility of producing transparent conductive oxide films through low-cost process. The optimum Ca doping concentration was 3.0 at.%, where the film resistivity was 2.3×10^{-3} Ωcm. The resistivity of the films was initially decreased with increasing Ca content up to 3.0 at.%, and then increased at higher doping concentration. All of the obtained films were polycrystalline with hexagonal structure and had a preferred orientation with the *c*-axis perpendicular to the substrate. Highly transparent films with a visible transmittance above 90% have been obtained with an optical band gap ranging from 3.31 to 3.36 eV. This work demonstrates the possibility of producing TCO Ca-doped zinc oxide films by rf-magnetron sputtering directly from aerogel nanopowder at room temperature.

Acknowledgement

This work has been financially supported by the Tunisian ministry of higher education, scientific research and technology and by the CMCU under contract n° 06/S1111.

References

[1] B. Szyszka, Thin Solid Films **351** (1999) 164
[2] K. Ellmer, J. Phys. D: Appl. Phys. **34** (2001) 3097
[3] E. M. Bachari, G. Baud, S. Ben Amor, M. Jacquet, Thin Solid Films **348** (1999) 165
[4] X. Jiang, F. L. Wong, M. K. Fung, S. T. Lee, Appl. Phys. Lett. 83 (2003) 1875
[5] Y. F. Lu, H. Q. Ni, Z. H. Mai, Z. M. Ren, J. Appl. Phys. **88** (2000) 498
[6] P. Petrou, R. Singh, D. E. Brodie, Appl. Phys. Lett. **35** (1979) 930
[7] P. Nunes, E. Fortunadeo, R. Martins, Thin Solid Films **383** (2001) 277
A. P. Roth, D. F. Williams, J. Appl. Phys. **52** (1981) 6685
[8] E. Jimenez-Gonzalez, A. Jose, R. Suarez-Parra, J. Cryst. Growth **192** (1998) 430
[9] Lidia Armelao, F. Monica Fabrizio, G. Stefano Gialanella, Z. Fiorenzo Zordan, Thin Solid Films **394** (2001) 90
[10] Z. Ben Ayadi, L. El Mir, K. Djessas, S. Alaya, Nanotechnology **18** (2007) 445702
[11] L. El Mir, Z. Ben Ayadi, M. Saadoun, H. J. Von Bardeleben, K. Djessas, A. Zeinert, Phys. Stat. Sol. (a) **204** (2007) 3266
[12] L. El Mir, Z. Ben Ayadi, M. Saadoun, K. Djessas, H. J. von Bardeleben, S. Alaya, Appl. Surf. Sci. **254** (2007) 570
[13] Z. Ben Ayadi, L. El Mir, K. Djessas, S. Alaya, Mater. Sci. Eng. C **28** (2008) 613
[14] Y. Chem, D. M. Bagnall, H. K. Koh, K. T. Park, K. Hiraga, Z. Q. Zhu, T. Yao, J. Appl. Phys. **84** (1998) 3912
[15] D. Cullity, *Elements of X-ray Diffraction*, Addison-Wesley, Reading, MA, (1978)
[16] S. Y. Kuo, W. C. Chen, F. I. Lai, C. P. Cheng, H. C. Kuo, S. C. Wang, W. F. Hsieh, J. Cryst. Growth **287** (2006) 78

[17] J. F. Chang, C. C. Shen, M. H. Hon, Ceram. Int. **29** (2003) 245
[18] S. Yamauchi, H. Handa, A. Nagayama, T. Hariu, Thin Solid Films **345** (1999) 12
[19] V. Musat, B. Teixeira, E. Fortunato, R. C. C. Monteiro, P. Vilarinho, Surf. Coat. Technol. **180-181** (2004) 659
[20] K. Ellmer, G. Vollweiler, Thin Solid Films **496** (2006) 104
[21] Y. Igasaki, H. Saito, J. Appl. Phys. **69** (1991) 2190
[22] J. I. Pankove, Optical Processes in Semiconductors, Dover, New York, (1976)
[23] E. Burstein, Phys. Rev. **93** (1954) 632
[24] T. S. Moss, Phys. Soc. Lond. B **67** (1954) 775